



PERGAMON

Continental Shelf Research 22 (2002) 1909–1934

---

---

CONTINENTAL SHELF  
RESEARCH

---

---

www.elsevier.com/locate/csr

# Assimilation of water level data into a coastal hydrodynamic model by an adjoint optimal technique

Aijun Zhang\*, Bruce B. Parker, Eugene Wei

*Coast Survey Development Laboratory (CSDL), National Ocean Service/NOAA, NICS13, 1315 East-West Highway, Silver Spring, MD 20910, USA*

Received 15 July 2001; accepted 8 March 2002

---

## Abstract

An adjoint data assimilation system has been developed to assimilate coastal subtidal water level data into a hydrodynamic model. In this system, a linear two-dimensional Princeton Ocean Model with an orthogonal curvilinear grid system is used as the forward model. The wind drag coefficient is used as a convenient control variable (approximately representing errors in the forecasting wind fields that are usually the primary cause of errors in model-produced water levels). The cost function is defined in terms of the water level misfits between the observations and model outputs. The limited memory Broyden–Fletcher–Goldfarb–Shanno (BFGS) quasi-Newton method for large-scale optimization is implemented to minimize the cost function. Identical twin experiments with model-generated pseudo-observations are performed and the results show that the true solution of the control variable can be recovered efficiently by assimilating pseudo-observations at limited locations into the model. The results from actual subtidal water level data assimilation experiments show that the simulated subtidal water levels with data assimilation are better than those without data assimilation even if only one control variable is used. The results from the experiment with 16 control variables demonstrate that the correlation coefficients are greater than 0.93 and the RMS errors are less than 5.3 cm at 18 coastal water level gauge stations. The nowcast/forecast experiments demonstrate that the subtidal water level forecasts are improved by water level data assimilation in the first 6 h. The average RMS error of the subtidal water level forecasts over the 18 water level gauge stations is reduced by 3 cm. Crown Copyright © 2002 Published by Elsevier Science Ltd. All rights reserved.

*Keywords:* Water level; Wind drag coefficient; Data assimilation; The US East Coast

---

## 1. Introduction

Water levels and currents play an important role in the coastal exploitation, navigation and management (for example, maritime traffic management, response to oil spills, fisheries, tourism,

recreational sports). Generally, two factors affect water level variation. The first factor is astronomical tides which are produced by the gravitational attraction of the moon and sun acting upon the rotating earth. The second is nontidal water level variation which is primarily generated by the surface wind, but also includes the effects of changing atmospheric pressure and changing water density (due to changing temperature and

---

\*Corresponding author. Fax: +1-301-713-4501.

*E-mail address:* aijun.zhang@noaa.gov (A. Zhang).

salinity). Astronomical tidal prediction has been studied for decades and tidal prediction using either harmonic or response technique is quite accurate in most cases. For over a century, mariners who needed information on water levels and currents have had to rely on astronomical tide and tidal current prediction tables. However, tide and tidal current predictions cannot tell mariners what the real water levels and currents will be in the future due to not including the often important effects of winds, river flow, atmospheric pressure, or water density. These nontidal effects could sometimes be significant and completely overwhelm the tidal signal. Real-time observing systems provide mariners with instant information on the total water levels and currents which is more accurate than tidal predictions, but such information cannot be provided into the future nor at locations other than those that are instrumented.

Numerical models have been widely applied to simulations of coastal ocean circulation. Several marine nowcast/forecast model systems for coastal zones and estuaries have been developed and are running in experimental mode: Coast Ocean Forecast System (Aikman et al. 1996); Experimental Real-Time North Pacific Ocean Nowcast/Forecast System (Kuo, personal communication); Lower Columbia River Nowcast/Forecast Systems (Baptista et al., 1998); Chesapeake Bay Operational Forecast System (Gross et al., 2000). These nowcast/forecast model systems not only provide water level forecast at particular locations, but they also have the advantage of providing spatially varying two-dimensional water level forecasts, and/or three-dimensional current forecasts. Sensitivity experiments using numerical models are also helpful for researchers to understand the physical oceanographic dynamics of some special phenomena. However, even the highest resolution ocean circulation model cannot resolve all of the dynamically important physical processes in the ocean. There are always some processes that are not represented directly (Malanotte-Rizzoli and Tziperman, 1996), but rather are parameterized. These tunable parameters (i.e. various eddy coefficients, surface wind drag coefficients, bottom

friction coefficients, etc.) are always uncertain both in form and value. Many of the parameters are also often difficult to measure directly. However, oceanographic data in the interior of the domain can be used to help estimate the undetermined parameters. The combination of a model and data for determination of the poorly known model parameters and for improvement of the ocean model performance can be formulated as an optimization problem. Such an optimization would search for a set of model parameters and for an optimal ocean state which together satisfy the model equations and fit the available data as well as possible. This may be done by formulating a cost function, which represents the differences between the model results and the observations. The cost function is minimized, with the model governing equations as strong constraints, by adjusting the control variables using unconstrained optimization algorithms (such as the conjugate gradient method and the limited memory quasi-Newton method) which require the gradients of the cost function with respect to the control variables. The estimation of these parameters therefore becomes an extremely complicated optimization problem which needs to be carried out using efficient methods and powerful computers.

In recent years, the adjoint technique has been developed and widely applied in meteorological and oceanographic fields, especially for data assimilation, model tuning, model sensitivity analysis, and parameter estimation. The adjoint approach with the governing equations as strong constraints was described by Sasaki (1970), who gave a framework that is readily applicable to a set of steady- or unsteady-state equations. Bennett and McIntosh (1982) and Bennett (1985) used the adjoint variational method to determine the open boundary conditions in a tidal model and array design. Yu and O'Brien (1991, 1992) used the adjoint method in a one-dimensional vertical model to estimate the wind stress drag coefficient, the oceanic eddy viscosity profile, and initial conditions from observed velocity observations. Panchang and O'Brien (1989) applied the adjoint variational method to a one-dimensional hydraulic model to determine the bottom friction

coefficients in a tidal river. Das and Lardner (1991) and Lardner (1993) implemented the adjoint method for a two-dimensional tidal model to determine the bottom friction coefficients and water depths from periodic tidal data. Similarly, Lardner et al. (1993) estimated the bottom drag coefficient and bathymetry correction for a two-dimensional tidal model of the Arabian Gulf. Lardner and Song (1995) used the adjoint method in the optimal estimation of viscosity and friction coefficients for a quasi-three dimensional numerical tidal model. Seiler (1993) used the adjoint method to estimate open boundary conditions for a quasi-geostrophic ocean model.

Those studies about the adjoint technique are mainly concerned with studying the method rather than applying it to real oceanic conditions and operational oceanic nowcasts/forecasts. In this study, we develop the adjoint model of the two-dimensional linear Princeton Ocean Model (POM), and apply it to subtidal water level data assimilation. The assimilated data consists of water levels at 18 water level gauge stations along the US East Coast. Since the surface wind has the predominant effect on the subtidal water level variation along most of the US East Coast, wind drag coefficients are chosen as the control variables. (This is merely a convenient way to correct water level differences due to errors in the forcing wind fields, and should be viewed as a first step in a water level assimilation methodology. This simplification forces other errors, e.g., in the barometric pressure, water temperature, etc., to be treated as wind field errors.) The forward equations and the adjoint equations of the two-dimensional POM are described in Section 2. In order to verify and evaluate the adjoint model, identical twin experiments are conducted and the corresponding results are presented in Section 3. The application of the adjoint model to actual observed East Coast subtidal water level data is described in Section 4. Section 5 presents the results of the subtidal water level forecasts by including the water level data assimilation technique in the nowcast/forecast system and conclusions are described in Section 6.

## 2. Numerical model

### 2.1. Forward model

The adjoint method requires substantial computer resources to perform numerical computation. In order to make the operational real-time water level nowcast/forecast system as efficient as possible, the barotropic two-dimensional POM (Blumberg and Mellor, 1987) is linearized by: (1) neglecting the variation of water level surface elevation  $h$  relative to water depth ( $D = H$ ), which is reasonable for the depths over most of model regime; (2) neglecting the horizontal advection and diffusion terms ( $F_x$  and  $F_y$ ); (3) linearizing the bottom friction terms (which is also reasonable for the depths over most of the regime) with a constant bottom friction coefficient,  $C_b = 10^{-3}$ . Thus, the linearized two-dimensional continuity and momentum governing equations are as follows:

$$\frac{\partial h}{\partial t} + \frac{\partial HU}{\partial x} + \frac{\partial HV}{\partial y} = 0, \quad (1)$$

$$\frac{\partial HU}{\partial t} - fHV + gH \frac{\partial h}{\partial x} + C_d |W_s| W_u - C_b U = 0, \quad (2)$$

$$\frac{\partial HV}{\partial t} + fHU + gH \frac{\partial h}{\partial y} + C_d |W_s| W_v - C_b V = 0, \quad (3)$$

where  $h$ ,  $U$  and  $V$  are surface elevation and horizontal velocities,  $f$  is the Coriolis parameter,  $H$  is the water depth at rest,  $C_d$  is the wind drag coefficient,  $W_s$  is the surface wind speed, and  $W_u$  and  $W_v$  are surface wind components in the  $x$  and  $y$  directions.

An orthogonal curvilinear horizontal model grid (Fig. 1) with resolution ranging from 5 km near the coast to 30 km in the deep waters is implemented. The bathymetry in the model domain (shown in Fig. 2) is based on the DBDB5 (National Geophysical Data Center, 1985) gridded 5' bathymetry except in coastal regions (water depth less than 200 m) where the NOS15 gridded 15" (National Geophysical Data Center, 1988) bathymetry data are used because of better resolution and accuracy of bottom topography and coastal geometry.

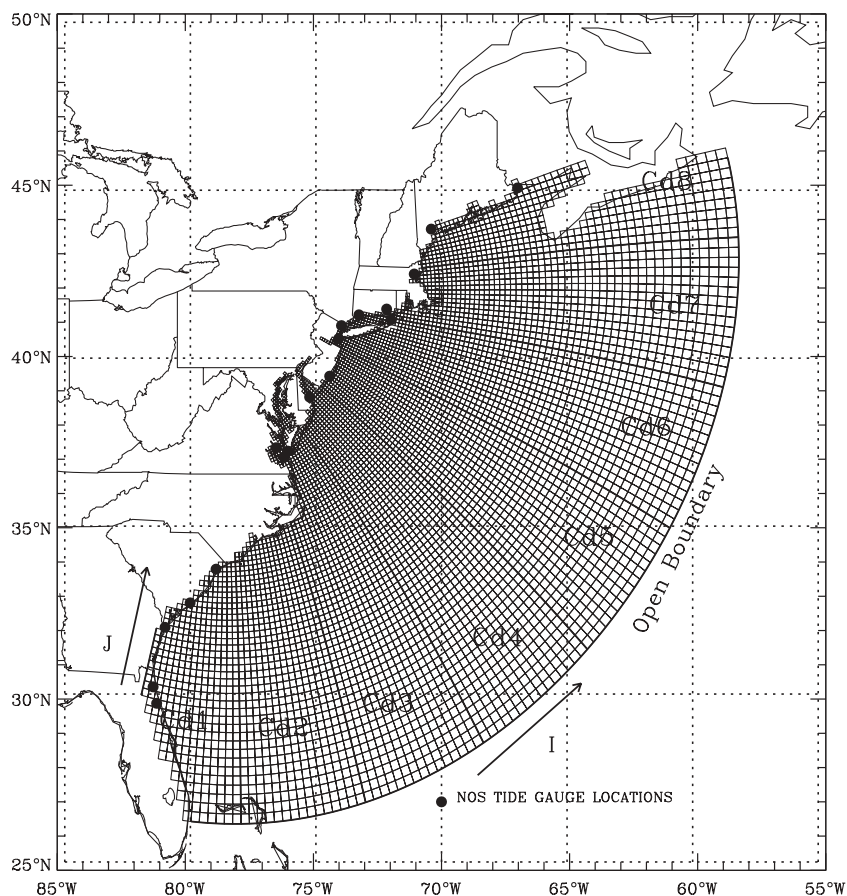


Fig. 1. Model grid.  $I$  and  $J$  are horizontal grid index in the  $x$  and  $y$  directions, respectively.

The model is driven by surface atmospheric pressure and Eta Data Assimilation System (EDAS)-analyzed surface wind fields (Black, 1994; Rogers et al., 1995) which are bilinearly interpolated to the model grid.

## 2.2. Cost function and control variables

The optimal adjoint method attempts to find a set of undetermined parameters (i.e., control variables) to minimize the cost function in a least-squares sense over a given period of time (the window of data assimilation). Thus, the first task is to define a suitable cost function for a given problem. In a general sense, the cost function measures the differences between the observations

and the numerical model results. With the increasing ability to acquire real-time water level observations along the coast, it is feasible to assimilate real-time observed water levels into a numerical model to improve water level nowcasts and the forecasts initialized with those nowcasts. In this study, we focus on how well the simulated subtidal water levels can be improved by assimilating the observed subtidal water levels into the numerical model using an optimal control data assimilation technique. According to the studies of Courtier and Talagrand, 1990, Zou et al. (1992) and Lardner et al. (1993), it is necessary to add penalty terms in the cost function expression to suppress the high-frequency variations in the state variable simulations and solution of the optimal

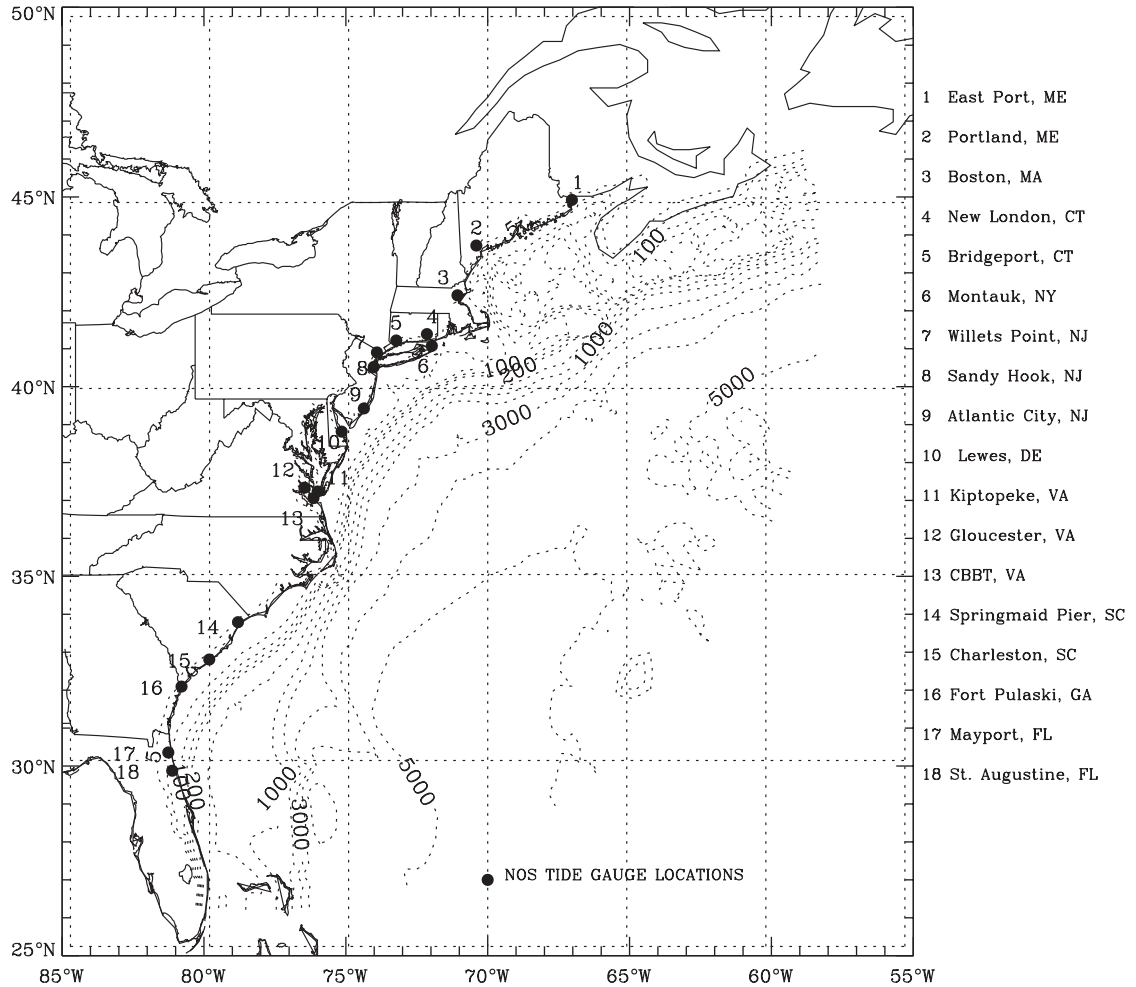


Fig. 2. Bathymetry in the model domain (in meters) and water level gauge locations from the National Water Level Observation Network.

control variables. The cost function is therefore defined as

$$\begin{aligned}
 J = & \frac{1}{2} \sum_{n=2}^N \sum_{i=1}^M W_i (h_{m_i}^n - h_{o_i}^n)^2 + \frac{1}{2} \gamma_1 \sum_{k=1}^{N_c} (C_{d_k} - C_{d_k}^p)^2 \\
 & + \frac{1}{2} \gamma_2 \sum_{k=1}^{N_c-1} (C_{d_{k+1}} - C_{d_k})^2, \quad (4)
 \end{aligned}$$

where  $h_{o_i}^n$  and  $h_{m_i}^n$  are observed and simulated subtidal water levels at time step  $n$  of the  $i$ th tide gauge;  $W_i$  is the corresponding weighting factor

(taken as 1.0 in this study) and  $M$  is the number of observation stations. The second and third terms are the penalty terms which measure the variances in time and space of the optimal  $C_d$ .  $C_d$  and  $C_d^p$  are the new and previous control variable values,  $N_c$  is the total number of the control variables, and  $\gamma_1$  and  $\gamma_2$  are weighting coefficients which represent the relative influence of these penalty terms and are empirically determined.

From sensitivity experiments, we found that the surface wind forcing has a predominant effect on the low-frequency subtidal water level variations

along the East Coast. We have therefore chosen the wind drag coefficient as a convenient control variable in the optimal adjoint data assimilation process. This selection essentially assumes that errors in the model-produced subtidal water levels will most likely be due to errors in the wind stress field and that these wind field errors can be approximately represented by changes in the wind drag coefficients. This simple approach forces other (usually much smaller) errors in water level, e.g., caused by errors in the barometric pressure, water temperature, etc., to be treated as though they were caused by wind field.

There may really be errors in model-based-analyzed or -forecasted wind fields. Fig. 3 shows a comparison between the observed winds and the EDAS winds interpolated to the corresponding model grid points of Eastport, CBBT, Duck and Cape Hatteras. It shows that, in general, the EDAS winds match the observed winds in speed and direction reasonably well at CBBT, Duck, and Cape Hatteras and less well at Eastport during this period. The EDAS wind speed is smaller than the observational wind speed and the direction deviates from the observation during the strong wind periods. The wind direction deviation plays an important role in variation of subtidal water level along the East Coast, which is very sensitive to wind direction. Wind observations from a moored buoy 44014 (at 36.58N, 74.83W), which is located very close to CBBT, were also compared with the EDAS interpolated winds. The results also showed that the EDAS wind direction deviates from the buoy measured wind, and the wind speed of the buoy observation is greater than that of the EDAS winds during the strong wind events. In addition to the errors in surface wind fields, it is possible that there really could be errors in the wind drag coefficient, since its behavior as wind speed increases is still not well understood, especially at high wind speeds. A problem with the wind drag coefficient can also occur if the effect of atmospheric stability is not included in its formulation, in which case, changing air and water temperature could affect wind stress in an unaccounted manner.

The most widely applied wind stress formulation at the sea surface may be conveniently expressed in terms of the wind speed at the 10-m

level, the air density, and a nondimensional drag coefficient as

$$\vec{\tau}_s = \rho_a C_d |\vec{W}_{10}| \vec{W}_{10} \quad (5)$$

for the formulation developed by Large and Pond (1981),

$$10^3 C_d = \begin{cases} 1.2 & 4 \leq |\vec{W}_{10}| \leq 11 \text{ m/s,} \\ 0.49 + 0.065 |\vec{W}_{10}| & 11 < |\vec{W}_{10}| \leq 25 \text{ m/s.} \end{cases} \quad (6)$$

The problem of evaluating the surface wind stress is therefore reduced to estimating the drag coefficient,  $C_d$ , at different wind speeds if the 10-m level winds and air density are known. Most estimates of  $C_d$  have been obtained by indirect observations. The dependence of  $C_d$  on wind speed has not been completely resolved, even for the lower wind speed. Thus, in this study, by assimilating the observed subtidal water level into the numerical model, it is possible to improve the wind stress field estimates by adjusting the wind drag coefficient  $C_d$ , to produce the most accurate simulated subtidal water levels.

Eq. (6) shows that surface wind drag coefficient is a temporally and spatially variable parameter (since wind speed varies in time and space). However, due to the limitation of available water level stations (number and spatial distribution), the wind drag coefficient is assumed to be constant in space, in each of one or more pieces of the model domain within 24 h. Since order of magnitude of  $C_d$  is about  $10^{-3}$ , for the purpose of convenience and computational accuracy,  $C_d$  is scaled by a factor of  $10^{-3}$  (i.e., the scaled  $C_d^* = C_d \times 10^3$ ). Hereafter, the scaled  $C_d^*$  is still written as  $C_d$ .

### 2.3. Adjoint equations

The adjoint method is efficient for calculating the gradient of a cost function with respect to control variables. Since the adjoint model is dependent on the forward model and its discretization method, the construction of an adjoint model seems very complicated (e.g., POM usually employs orthogonal curvilinear grid and several smoothing techniques in time and space discretization). The adjoint model equations can be derived

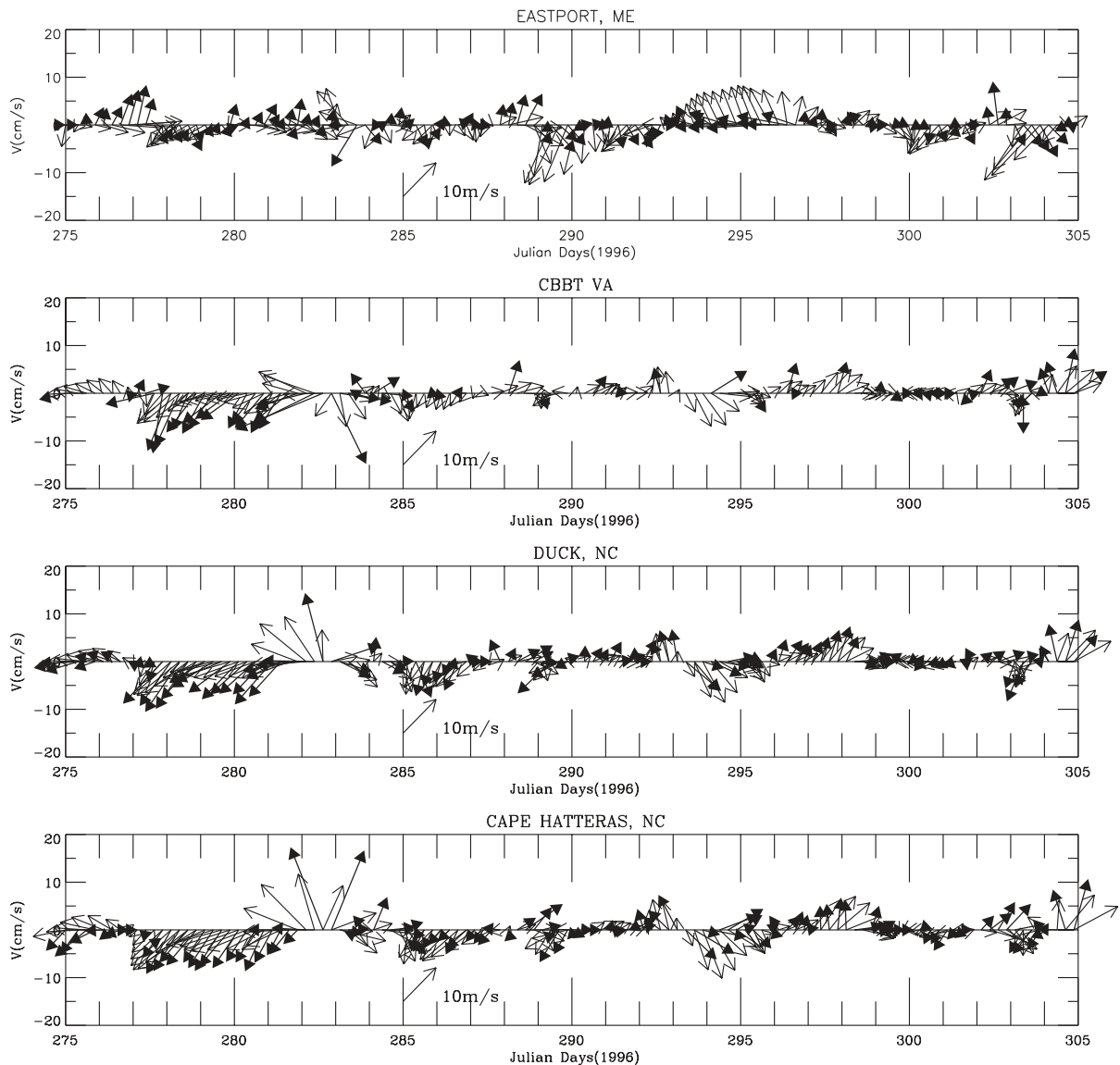


Fig. 3. Comparison of the observed and EDAS-analyzed surface winds at Eastport, CBBT, Duck and Cape Hatteras in October, 1996. Solid arrows, observations and open arrows, EDAS-analyzed surface winds.

by different methods: the Euler–Lagrange method (Morse and Feshbach, 1953); the control theory method (Le Dimet and Talagrand, 1986); and the Lagrange multiplier approach. Discrete adjoint equations can be derived by discretizing the continuous adjoint equations, or derived directly from

the discrete forward numerical model code. The direct derivation of adjoint discrete equations from model code can avoid the inconsistency that may arise from the derivation of the adjoint model by discretization due to noncommutativity of the adjoint model and discretization operations (Spitz, 1995).

In this study, we develop the discrete adjoint model of the linear two-dimensional POM directly from its discrete model equations using the Lagrange method. A complete derivation of the adjoint equations is very lengthy and can be found in Zhang et al. (2002). For clarity, we write the adjoint equations and gradient formulation here in continuous notation as

$$H \frac{\partial \lambda_u}{\partial t} - fH\lambda_v + H \frac{\partial \lambda_h}{\partial x} + C_b\lambda_u = 0, \quad (7)$$

$$H \frac{\partial \lambda_v}{\partial t} + fH\lambda_u + H \frac{\partial \lambda_h}{\partial y} + C_b\lambda_v = 0, \quad (8)$$

$$\frac{\partial \lambda_h}{\partial t} + g \left( \frac{\partial H\lambda_u}{\partial x} + \frac{\partial H\lambda_v}{\partial y} \right) = W_i(h - h_o). \quad (9)$$

The corresponding adjoint variables are defined as follows:  $\lambda_h$  is the adjoint variable of  $h$ ,  $\lambda_u$  is the adjoint variable of  $U$ , and  $\lambda_v$  is the adjoint variable of  $V$ , respectively. The gradient of cost function with respect to the control variable is given as

$$G = \frac{\partial J}{\partial C_{dk}} = \lambda_u |W_s| W_u + \lambda_v |W_s| W_v + \gamma_1 (C_{dk} - C_{dk}^P) - \gamma_2 (C_{d_{k+1}} - C_{dk}), \quad (10)$$

$$k = 1, \dots, N_c.$$

By comparison between the forward and the adjoint equations, it can be found that the adjoint equations have the following properties: (1) no wind forcing terms are included in the adjoint equations because the wind drag coefficients are used as the control variables; (2) data misfits are added to the adjoint equations as forcing terms; and (3) the adjoint equations are similar to the forward model equations, but the bottom friction terms in the adjoint equations have opposite signs to that of the corresponding governing equations. This implies that the adjoint equations have to be integrated backward in time. Note that no matter how many control variables are there in the adjoint data assimilation scheme, the gradient components of the cost function can be computed after integrating the adjoint model once. The adjoint equations demonstrate that the adjoint model integration has an approximately equivalent computational expense as the integration of its

forward model. Thus, the adjoint model provides an efficient method for calculating gradient components of a cost function which are used in the optimization process, especially for the case with the large number of control variables.

The following procedure of the iterative optimal data assimilation scheme which is applied to all the following data assimilation experiments is described as:

- (i) Run the forward numerical model for 24 h (data assimilation window is set to be 24 h in the present study) with initial values of the control variables, and save the simulated elevations at the corresponding tidal gauge locations at each hour.
- (ii) Calculate the data misfits and cost function.
- (iii) Run the adjoint model backwards in time forced by data misfits to calculate the adjoint variables  $\lambda_h$ ,  $\lambda_u$ ,  $\lambda_v$ , and then calculate the gradient of the cost function with respect to the control variables.
- (iv) Employ the limited memory Broyden–Fletcher–Goldfarb–Shanno (BFGS) quasi-Newton minimization algorithm (Liu and Nocedal, 1989) to calculate the optimal control variable estimates.
- (v) Check whether the convergence criterion,  $|G| < \varepsilon$  or  $J < \varepsilon$  ( $\varepsilon = 10^{-6}$ ), is satisfied. If yes, the iteration is stopped. Otherwise, steps (i)–(v) are repeated with the new parameter estimates.
- (vi) Rerun the forward numerical model with the optimal wind drag coefficients.

### 3. Model verification

The performance of a forward model (which should include all dynamical processes) is very important to a data assimilation system. In order to evaluate the linear numerical model and compare with the nonlinear two-dimensional POM, the linear and nonlinear numerical models were integrated with the same surface wind forcing for the period of 09/01–31/12/1996, during which there were several hurricanes and storm events. The simulated wind-driven (hereafter called

subtidal) water levels (in Fig. 4) show that the differences of the simulated subtidal water levels between the linear and nonlinear models are insignificant in this model domain. The sensitivity experiments demonstrate that the differences in the simulated subtidal water levels along the East Coast between the linear and nonlinear numerical models are mainly caused by the linearization of the bottom friction terms. Impacts of the horizontal advection and diffusion terms on subtidal water level simulation are negligible. Therefore, it

is reasonable to implement the linear two-dimensional model as a more efficient replacement for the nonlinear one.

In comparison, the observed subtidal water levels (filtered by a 30-h Fourier low-pass filter) are also plotted in Fig. 4. The simulated subtidal water levels from the linear model are in good agreement with observations at most water level gauge locations. The RMS errors of the simulated subtidal water levels range from 8 to 15 cm. The correlation coefficients between the observed and

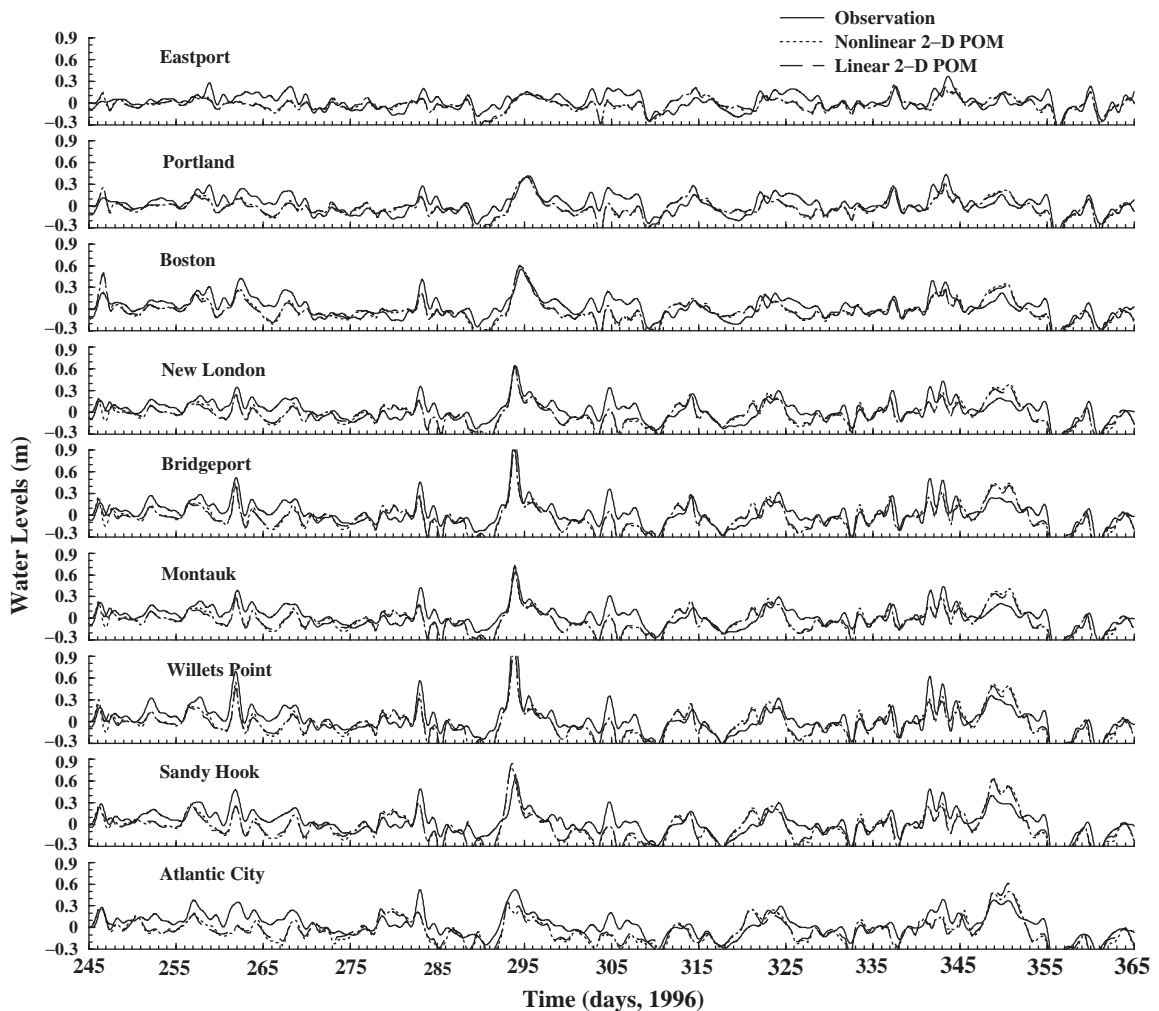


Fig. 4. Time series of observed and simulated subtidal water levels with the nonlinear and linear two-dimensional POM at water level gauge locations from 09/01 to 12/30/1996. See Fig. 2 for the locations.

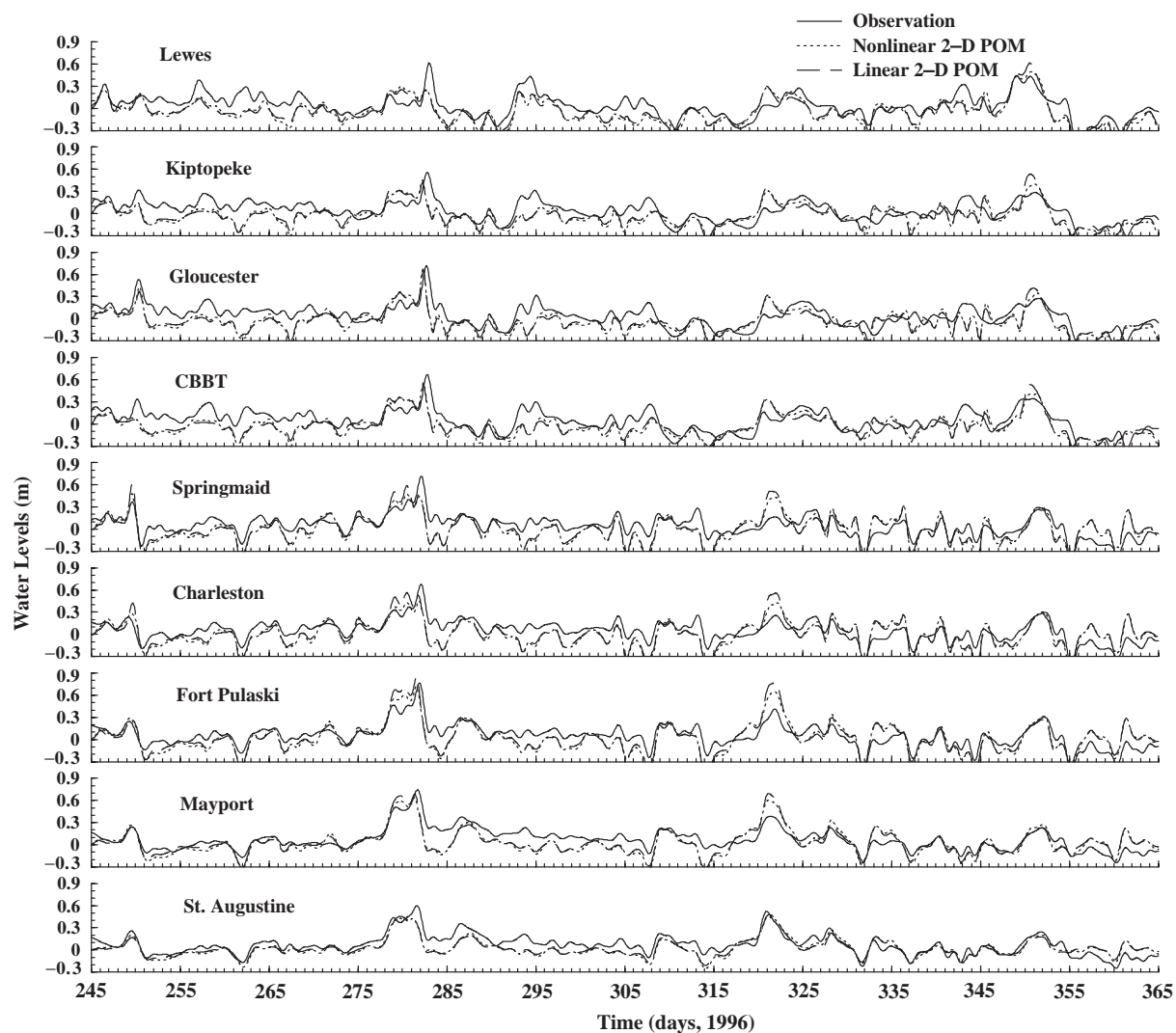


Fig. 4 (continued).

simulated subtidal water levels vary from a maximum of 0.91 at Willets Point and New London to a minimum of 0.54 at Cape Hatteras. Between Portland and Sandy Hook, the simulated subtidal water levels agree with the observed subtidal water levels very well during hurricane events. Near Cape Hatteras, the simulated subtidal water level does not follow the observations well. The latter result is consistent with those of Wang (1979) and Noble and Butman (1979), who pointed out that Gulf Stream effects contribute

to significant sea level fluctuations at Cape Hatteras.

In order to examine the response of subtidal water levels along the East Coast to surface wind, some model sensitivity experiments were performed with steady winds as forcing. The results show that, after reaching a steady ocean state, westerly and northwesterly winds push water away from coast and drop water levels over the continental shelf of the East Coast. Easterly and southeasterly winds pile water up and raise water

levels along the East Coast. Northeasterly winds can raise the water levels south of Atlantic City and lower the water levels north of Atlantic City. Southeasterly winds lower the water levels south of Atlantic City and raise the water levels north of Atlantic City. Southerly winds raise the water levels north of Cape Hatteras and lower the water levels south of Cape Hatteras. The comparison of the observed subtidal water levels with wind observations (Figs. 3 and 4) shows that easterly and northeasterly winds dominate at CBBT, Duck and Cape Hatteras from Julian days 280 to 282, water is therefore piled up at CBBT. After that, the wind becomes westerly and northwesterly which lowers the water levels.

The correctness of an adjoint code and the converging rate of the optimization process are critical to the success of an adjoint model. Any error in the adjoint model code can result in wrong information for computations of the gradient of the cost function, and then the optimization process may fail to find a reasonable optimal parameter estimation. Therefore, the code of the adjoint model must be verified to ensure that the gradient of the cost function is correctly calculated by the adjoint model. The most useful method is to use gradient of the cost function to check the correctness of the adjoint model equations. This involves perturbing each of the control variables by an appropriate small amount  $\Delta C_d$  and integrating the forward model to calculate the change in the cost function with respect to the corresponding control variable. The derivative of the cost function at any point of  $C_d$  of the parameter space can be calculated by a finite-difference (FD) method. The gradient calculated from an adjoint model should be consistent with that calculated using the FD method within the order of  $\Delta C_d$ . The number of the control variables is limited due to the limitations of the number and spatial distribution of the available water level stations in this study and computational cost. Three cases are therefore considered: one with one control variable, one with eight control variables, and one with 16 control variables. For the one control variable case, the wind drag coefficient is specified as a constant over the entire model domain within a data assimilation window (24 h). For the eight

control variable case, the model domain is evenly divided into eight subregions along the  $J$  direction of the model grid (see the thick lines in Fig. 1). The wind drag coefficient in each subregion stays constant within a data assimilation window and is counted as a control variable. For the 16 control variable case, as an extension of the eight control variable case, the wind drag coefficients in the  $I$  and  $J$  directions are expressed as two different control variables ( $C_{dx}$  and  $C_{dy}$ ) in each subregion. The penalty terms in Eq. (4) are not considered in the following twin experiments. The results from the gradient verification experiments of the three cases show that the gradients of the cost function computed using the FD method and the adjoint method are very close in magnitude and consistent in sign. For the case with eight control variables, the maximum difference of the gradient components between the FD method and the adjoint method during the 30 consecutive days is  $1.33 \times 10^{-3}$ , and the maximum gradient norm difference is  $1.44 \times 10^{-3}$ . This demonstrates that the adjoint model developed in this study can provide correct gradient information for the optimization process. The most useful tool to verify and evaluate the performance and feasibility of the adjoint data assimilation procedure is the identical twin experiment. In which, pseudo-observations are generated by the numerical model itself with a predetermined control variable so they are not contaminated by any error and contain the same dynamics as the numerical model, and any kind of the pseudo-observations can be sampled. Another merit of the identical twin experiment is that the true values of the control variables are already known, we therefore can examine whether or not the optimal control variables converge to their true values. Thus, the identical twin experiment is the best situation for data assimilation, and for that reason it is widely used to evaluate and verify the performance of a developed adjoint data assimilation system. A set of identical twin experiments using perfect and contaminated pseudo-observation is performed for the case with one, eight and 16 control variables, respectively. Similar results are obtained from these twin experiments as follows: (1) the values of the optimal  $C_d$  converge towards their true solutions very fast

during the first several iterations; (2) no matter how far the initial guesses of the control variables are away from their true solutions, the value of the cost function and the norm of the gradient drop rapidly in the first several iterations, and the values of the optimal  $C_d$  are very close to their true solutions after about 10 iterations and all of the optimal  $C_d$  components gradually converge to their true solutions; and (3) the noise added to the pseudo-observations has significant impacts on the control variable estimations of the optimization process, i.e., observational noise inhibits the optimal  $C_d$  from converging to their true solutions. The twin experiments demonstrate that “true” solutions of control variables can be efficiently recovered by assimilating coastal water level gauge data into a hydrodynamical model if other model parameters are perfect.

#### 4. Assimilation of real subtidal water level data

The identical twin experiments demonstrated that the true values of the wind drag coefficients can be recovered by assimilating the pseudo-observations into the numerical model. In this section, the same three cases as the identical twin experiments with one, eight and 16 control variables were performed to assimilate the real subtidal water levels from water level gauges along the US East Coast. And the results with data assimilation are compared with those without data assimilation ( $C_d$  computed using Eq. (6), and the experiment is denoted as PA\_NoDA).

##### 4.1. Data and numerical scheme

Hourly water level observations from 18 water level gauge stations of National Water Level Observation Network (NWLON) were filtered with a 30-h low-pass Fourier filter to remove the astronomical tidal signal to obtain the observed subtidal water levels. The EDAS-analyzed surface wind fields from the National Centers for Environmental Prediction (NCEP) in the National Weather Service (NWS) were used as surface forcing of the numerical model.

The forward model was first spun up for 10 days from rest with the wind drag coefficient  $C_d$  calculated from the formulation developed by Large and Pond (Eq. (6)) to create initial fields for the adjoint data assimilation system. The variational adjoint data assimilation was then continuously performed for 50 days (09/10–10/30/1996) with a 24-h data assimilation window. The optimal values of the  $C_d$  from the previous day were used as the initial guess for the following day's data assimilation. After obtaining the optimal  $C_d$  the forward model was reintegrated for 24 h with the optimal  $C_d$ . A new initial field was then created and saved at the end of each day, and is used as the initial condition for the following day's simulation.

##### 4.2. Data assimilation results without penalty terms

For the moment, the penalty terms in Eq. (4) are not considered. The time series of the optimal wind drag coefficients from three cases are presented in Figs. 5(a)–(c). For the case with one control variable (denoted as PA\_NoPT1), the optimal values of  $C_d$  vary from  $-5.0$  to  $6.0$ . The negative values of  $C_d$  indicate that the wind stress direction is changed to the opposite to that of the surface wind in order to minimize the cost function. For the case with eight control variables (PA\_NoPT2), the optimal values of  $C_d$  for each subregion varies with time and seems to be uncorrelated with the others. This may be caused by the definition of the eight control variables, but it is not unexpected since the changes in  $C_d$  are made to compensate for assumed errors in the wind fields. The absolute values of the optimal  $C_d$  are generally less than  $20.0$ . However, the variance of each optimal  $C_d$  is greater than that of the one control variable case. Some of the optimal  $C_d$  seems to be unreasonably large compared with the wind drag coefficients calculated with Eq. (6). However, the magnitude of the cost function is reduced significantly with the optimal  $C_d$  from this experiment. This may indicate that the magnitude and/or direction of the surface wind stresses are not accurate enough so that the numerical model cannot simulate the subtidal water level well compared with the observations. In order to

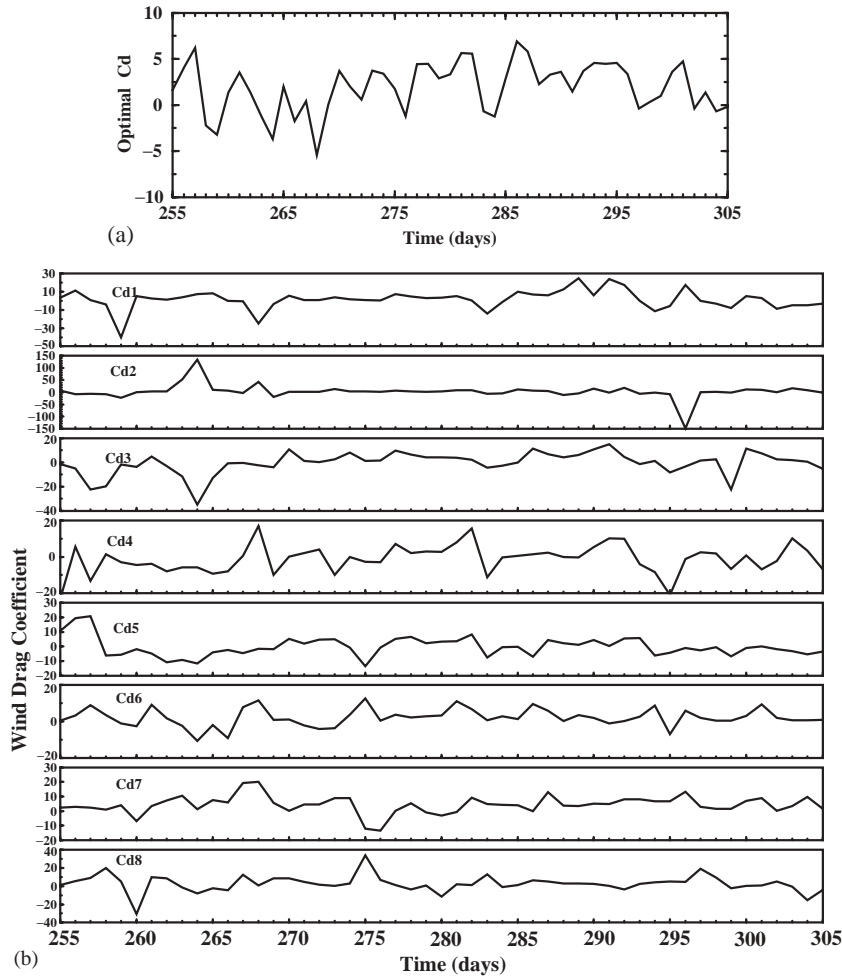


Fig. 5. (a) Time series of optimal values of  $C_d$  from the experiment PA\_NoPT1 (one control variable). (b) As Fig. 5a, but for the experiment PA\_NoPT2 (eight control variables). (c) As Fig. 5a, but for the experiment PA\_NoPT3 (16 control variables). (—)  $C_{dx}$ ; (---)  $C_{dy}$ .

minimize the cost function, wind stresses have to be adjusted by changing the wind drag coefficients which are used in the wind stress computation. For the case with 16 control variables (PA\_NoPT3), the optimal wind drag coefficient components  $C_{dx}$  and  $C_{dy}$  are not only different in magnitude but are also occasionally opposite in sign. From Eq. (5) we know that only when  $C_{dx}$  is equal to  $C_{dy}$  will the wind stress direction remain in the same direction with the surface wind. So the optimal  $C_{dx}$  and  $C_{dy}$  allow the wind stress direction calculated with the optimal  $C_{dx}$  and  $C_{dy}$  to deviate from that of the

surface wind. If both  $C_{dx}$  and  $C_{dy}$  are positive, the wind stress direction is off from the wind direction less than  $90^\circ$ . However, if  $C_{dx}$  and  $C_{dy}$  are both negative, the wind stress direction can be totally opposite to the wind direction.

Time series of the cost function for the three cases are presented in Fig. 6. In general, the values of the cost function with data assimilation are less than those without data assimilation, and the values of the cost function from 16 control variable case are smallest. This demonstrates that, in the sense of minimizing the cost function, the

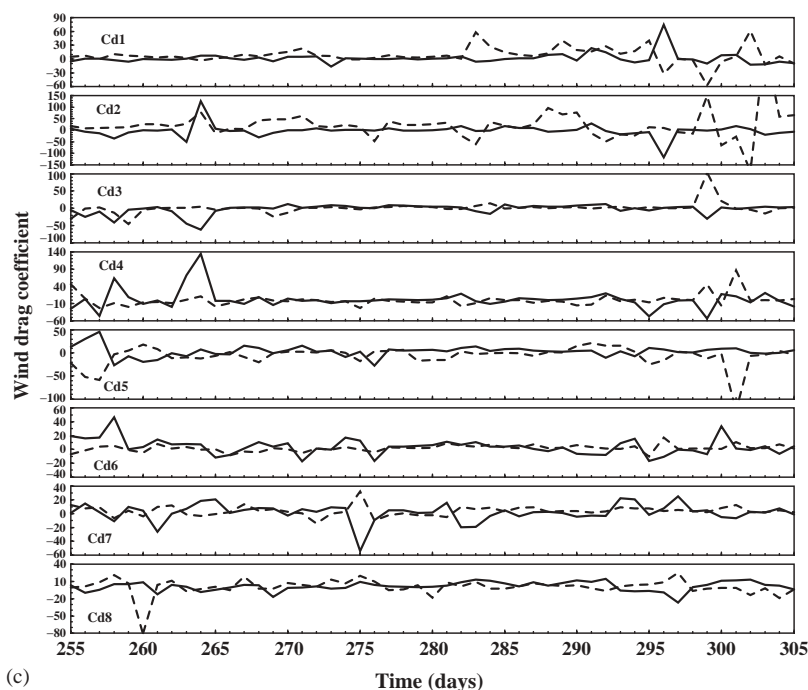


Fig. 5 (continued).

best results are obtained from the case with 16 control variables. It also indicates that allowing wind stress direction changes in the data assimilation procedure improves the accuracy of the simulated subtidal water level.

Time series of the subtidal water levels (Fig. 7) show that even if only one constant control variable in the entire model domain is used in the adjoint data assimilation process, the simulated subtidal water levels at 18 stations are closer to the observations than those without data assimilation. The results from PA\_NoPT2 show that the simulated subtidal water levels are much closer to the observed subtidal water levels than the results of the one control variable case. The simulated subtidal water levels from the 16 control variable case match the observations very well for most stations both in amplitude and phase, even during strong wind periods.

The correlation coefficients and RMS errors for the case without data assimilation and for the three cases with data assimilation are presented in Fig. 8. The correlation coefficients of the case

without data assimilation are the lowest and vary from 0.5 to 0.88. The correlation coefficients for the case with 16 control variables are the highest among these four cases and vary from 0.93 to 0.98. The RMS errors without data assimilation are the largest except at the St. Augustine station (which is already small) and vary from 6 to 14 cm. The RMS errors of the case with 16 control variables are the smallest and vary from 3.3 to 5.3 cm.

From wind drag coefficient laboratory experiment studies, we know that the wind drag coefficient is related to the wind speed, and therefore wind drag coefficient varies in space and time. Since we have allowed the changes of the optimal  $C_d$  to represent changes in the original winds to improve the simulated subtidal water levels along the coast, we can expect a variation in the calculated optimal values of  $C_d$  over space and time, and which will then be correcting for a variety of wind data problems (and possibly other problems as well). Since eight wind drag coefficients might represent the spatial variations of wind stress better than one control variable, the

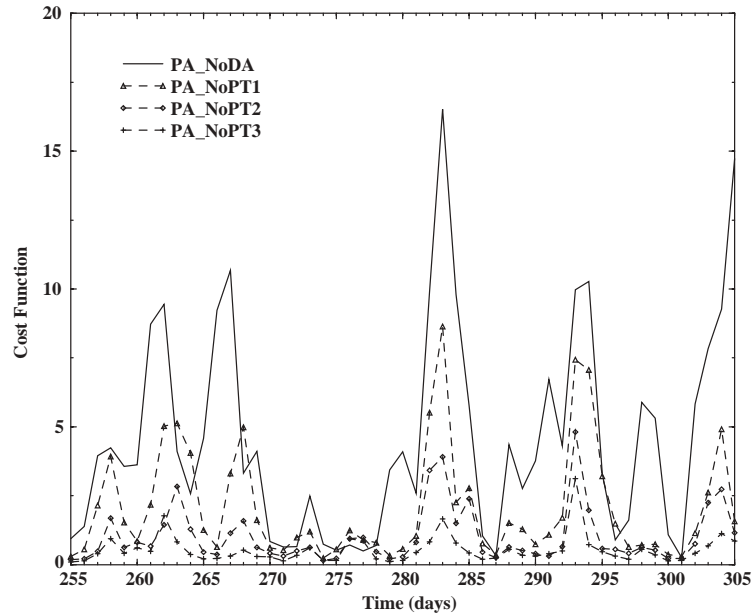


Fig. 6. Time series of cost function for the experiments with and without data assimilation.

simulated subtidal water levels from PA\_NoPT2 are closer to the observed subtidal water levels than that from PA\_NoPT1. In addition to optimizing the wind stress magnitude, 16 control variables also allow to adjust the wind stress direction by any angle (higher degree of wind correction compared with the eight control variable case), therefore the simulated subtidal water levels are further improved with respect to PA\_NoPT2. The more the control variables used in the data assimilation procedure, the better the results should be. However, it must also be noticed that more control variables require more observations to be assimilated into the model in order to obtain better optimal control variables, which, in turn, make the simulated results match the observations better. Only if there are adequate representative water level gauge stations, more control variables can be used in the data assimilation process. The relationship between the minimum number of stations and the number of control variables depends on the spatial and temporal distribution of the observations (Zhang et al., 2002) and could be examined with the identical twin experiments.

The results from the above experiments show that the values of the cost function with data assimilation decreased as expected. However, some optimal values of  $C_d$  appeared to be very large (for typical  $C_d$  values) and/or even negative, perhaps indicating a physically unrealistic solution. Such “abnormal” optimal values of  $C_d$  may be attributed to several possibilities: (1) There really are errors in the EDAS-analyzed wind fields (wind speed and wind direction, whatever the causes), and the wind field errors were corrected by changing the optimal wind drag coefficients (the negative value of  $C_d$  would be obtained if the wind direction was wrong). (2) Our inherent basic assumption has been that all errors in the simulated subtidal water levels are produced by the errors in the surface wind, and errors in the wind fields are corrected and represented by changes in wind drag coefficients. However, errors in the simulated water levels due to the other conditions and parameters (initial condition, open boundary condition, surface air-pressure field, nonlinear effects, and the other tunable parameters) will also be projected onto the control variables. This could result in an “abnormal”

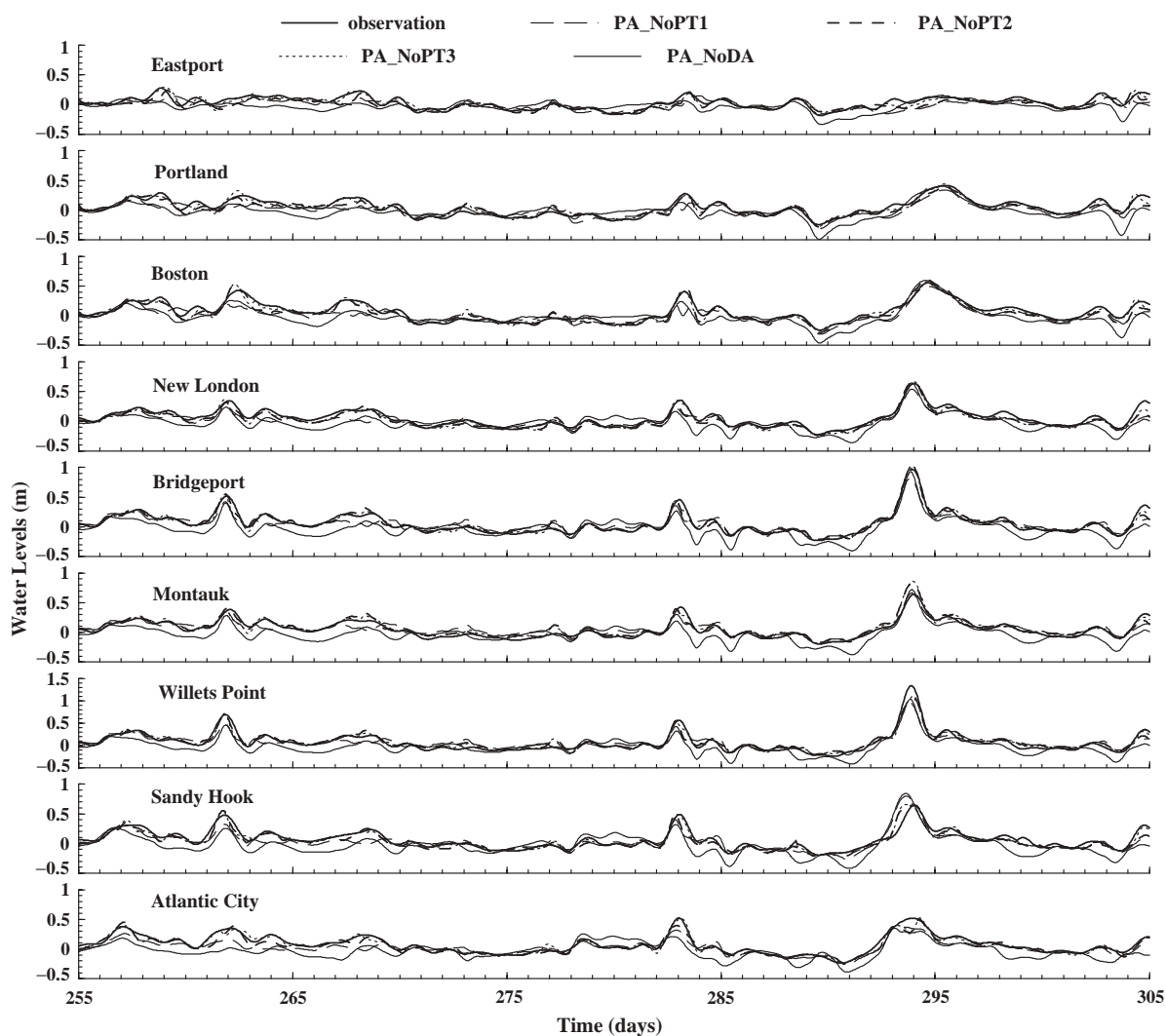


Fig. 7. Time series of the observed and simulated subtidal water levels with and without data assimilation.

value of the optimal  $C_d$  if the assumption was invalid. (3) Due to limitations in available water level stations,  $C_d$  is assumed to be constant, either throughout the entire domain (one control variable case) or in each subregion (eight and 16 control variable cases), but the true spatial variations of  $C_d$  may not be properly represented in the model. (4) The penalty terms are not considered. The minimization of the cost function alone does not ensure that the adjoint data assimilation technique obtains reasonable values

of the optimal control variable in the physical sense. The constraint conditions and penalty terms may be necessary to obtain more reasonable values of the optimal control variables.

#### 4.3. Effects of the penalty term and the smoothness of control variable

The purpose of adding the penalty term to the cost function is to smooth and stabilize the estimates of the control variables. The estimates

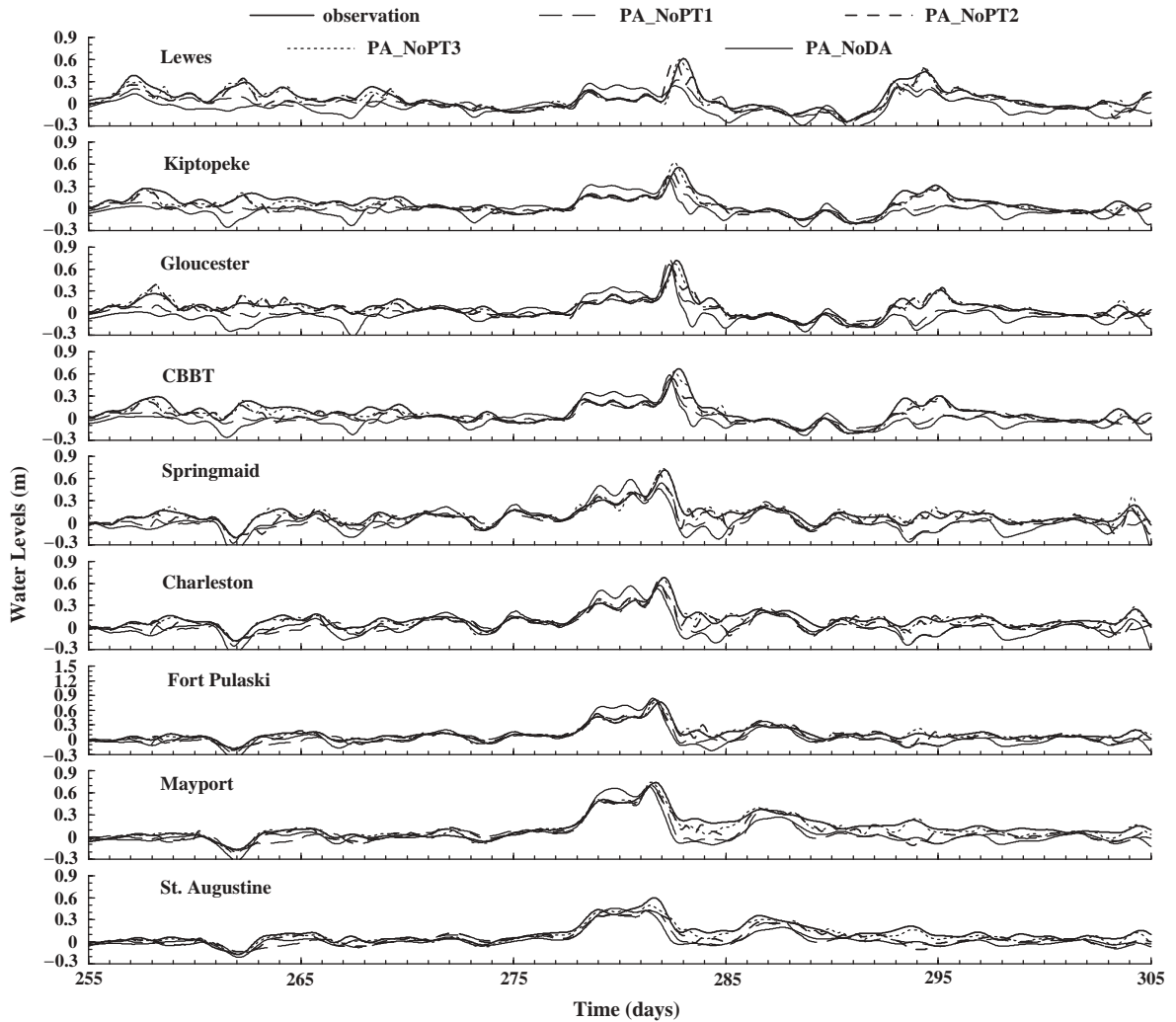


Fig. 7 (continued).

of the control variables from the cost function without penalty terms are indeed solutions satisfying the desired objective of minimizing the misfits between the model output and the observations, but they are rapidly varying in space and time. Thus, they are probably not desired solutions in physical and realistic respects. Our goal is to seek a balance between the misfit minimization and the solution smoothness. The first objective must dominate the latter, and the role of the smoothing terms must be kept to a minimum so that the real

structural features of the estimated control variables can be preserved to the greatest extent. The influences of these two objectives are regulated through the weighting coefficients. Therefore, two penalty terms are added in the cost function formulation with weighting coefficients  $\gamma_1$  and  $\gamma_2$ . Three additional experiments using 16 control variables were performed with different weighing coefficients (see Table 1 for the values of  $\gamma_1$  and  $\gamma_2$  for the three cases: PA\_PT1, PA\_PT2, and PA\_PT3), and the corresponding results are

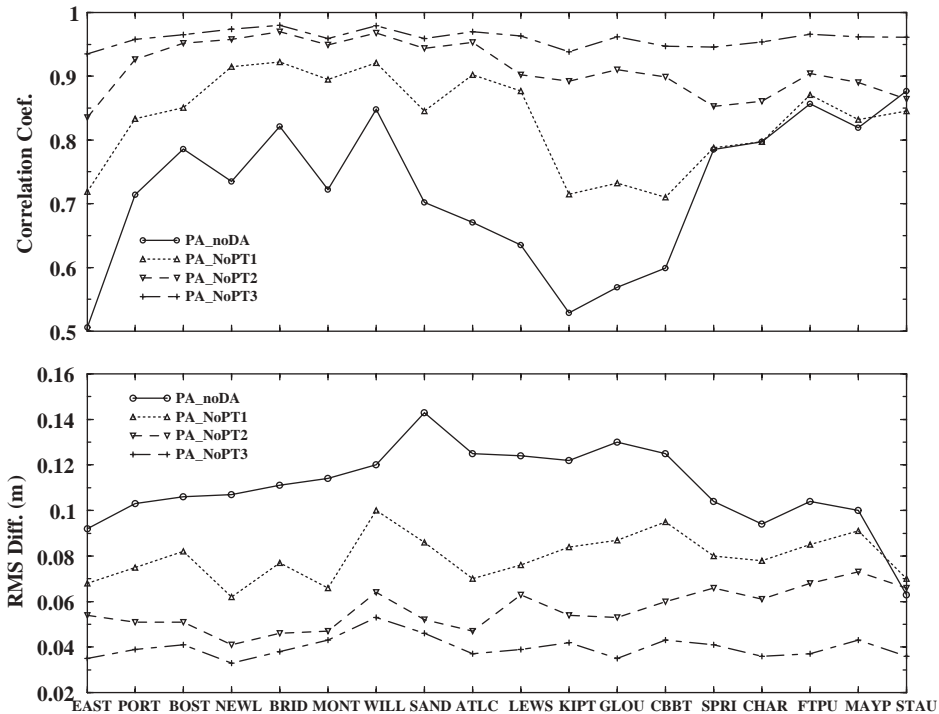


Fig. 8. Comparison of correlation coefficients and RMS errors between the observed and simulated subtidal water levels from the experiments with and without data assimilation.

Table 1  
Weighting coefficients of  $\gamma_1$  and  $\gamma_2$

Case name	$\gamma_1$	$\gamma_2$
PA_NoPT3	0.0	0.0
PA_PT1	0.001	0.001
PA_PT2	0.0025	0.0025
PA_PT3	0.005	0.005

compared with those from the experiment PA\_NoPT3 without penalty terms.

Time series of the optimal  $C_{dx}$  (similar results for  $C_{dy}$ ) from the four experiments are shown in Fig. 9. It can be seen that the time series of the optimal  $C_{dx}$  from the three experiments with penalty terms are very similar, and they are much smoother than that without penalty term (PA\_NoPT3). With the penalty terms, the spatial and temporal variations of the optimal  $C_{dx}$  are smoothed, and the extremely large values in the

optimal  $C_{dx}$  were eliminated. Thus, adding the penalty terms to the cost function appears to lead to a more physically realistic depiction of the optimal wind stress fields. Fig. 10 shows that, with the penalty terms, the correlation coefficients decrease and the RMS errors increase at the water level gauge stations. The differences of correlation coefficients and RMS errors between the cases with and without penalty terms are no more than 0.1 and 2 cm, respectively. This indicates that the realistic structural features of the subtidal water levels are preserved, while the estimated optimal values of  $C_d$  are smoothed. According to our experiment results, the most acceptable results would be those obtained from PA\_PT1 (using the smallest  $\gamma_1$  and  $\gamma_2$ ), since almost same pattern of the optimal  $C_d$  is obtained as that from PA\_PT2 and PA\_PT3 but the RMS errors are closest to that without penalty terms (although not very close for stations CBBT, Springmaid and Charleston). It is worth noting that the iteration number for each

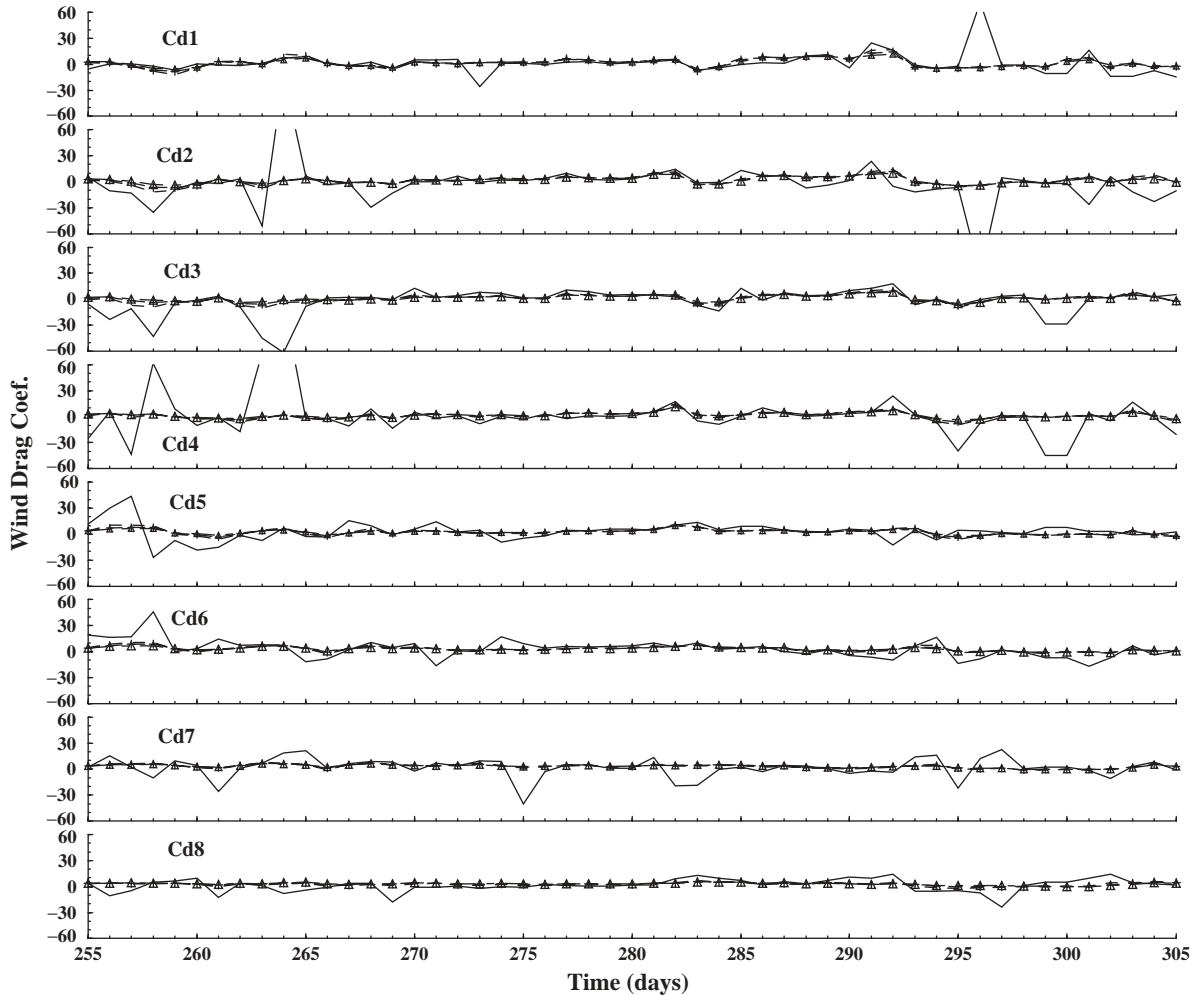


Fig. 9. Time series of optimal values of  $C_d$  for the data assimilation experiments with penalty terms. (—) PA\_NoPT3; (---) PA\_PT1; (+---+) PA\_PT2; and ( $\Delta$ --- $\Delta$ ) PA\_PT3.

24-h data assimilation is reduced by 50% with the addition of the penalty terms, thus reducing the model computational time. The effects of the penalty terms on subtidal water level forecasts will be discussed in the following section.

## 5. Subtidal water level forecasts

One important purpose of the data assimilation scheme is to improve subtidal water level forecasts in the coastal region by providing better initial

conditions for the forecasting model. Therefore, a 24-h nowcast/forecast system is configured. In this system, the forward model is run for 10 days to create restart files for the first nowcast/forecast run. The nowcast model is run for 24 h (forced by the EDAS-analyzed wind fields) to create an initial field for the forecast model. The forecast model is then run for the next 24 h forced by Eta forecast wind fields from NCEP/NWS from the initial fields created by the nowcast model. It is noted that the forecast model utilizes the same model grid, bathymetry and open boundary condition

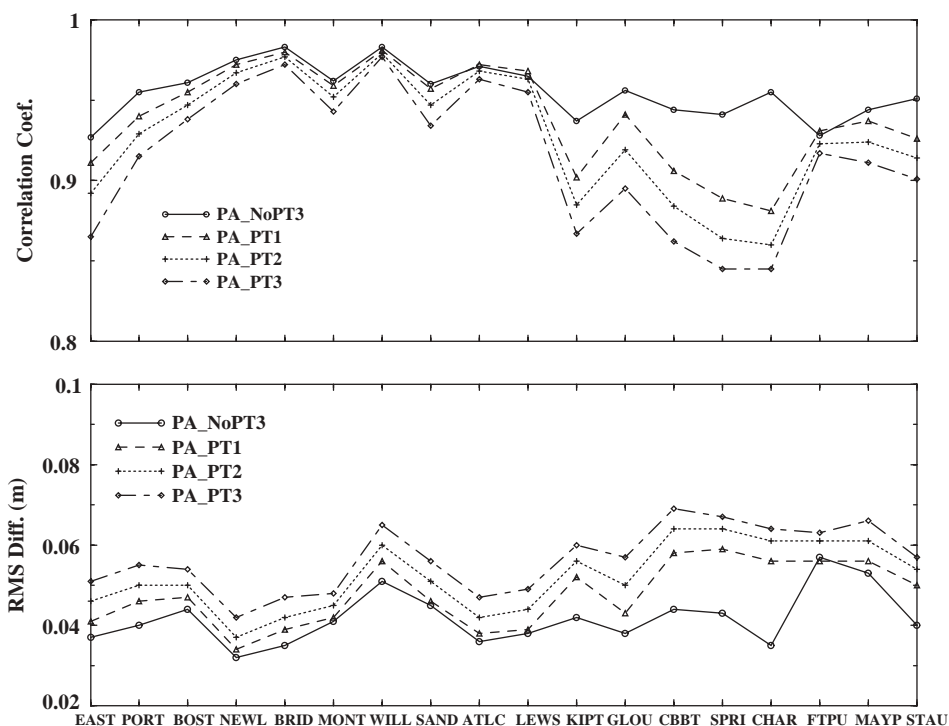


Fig. 10. Correlation coefficients and RMS errors between the observed and simulated subtidal water levels from the data assimilation experiments without penalty terms (PA\_NoPT3) and with three different weighting size penalty terms (PA\_PT1, PA\_PT2, and PA\_PT3). See Table 1.

formulations as the nowcast model. The five nowcast/forecast experiments (Table 2) were devised and continuously performed for the period from 09/11/1996 to 12/31/1996 (110 days), and the subtidal water level forecasts are used in the statistical analysis.

We are concerned with how much improvement of the subtidal water level forecasts is made by using the data assimilation technique in the nowcast/forecast system and how long the improvement could last. The subtidal water level forecasts for each hour of a 24-h forecast cycle over the 110-day period are sampled (110 data point for each forecast hour) and compared with the corresponding observations. The variations of the average correlation coefficient and RMS error over the 18 stations with forecast time for these experiments are presented in Fig. 11. For the experiment without data assimilation (SWL\_F1), the average RMS errors vary with forecast hour in the range from 9.8 to 13 cm. The average correla-

Table 2  
Wind drag coefficients used in the nowcast and the forecast modes for subtidal water level nowcast/forecast experiments

Case name	$C_d$ for nowcast mode	$C_d$ for forecast mode
SWL_F1	Eq. (6) (no data assimilation)	Eq. (6)
SWL_F2	Optimal $C_d$ from PA_NoPT3	Eq. (6)
SWL_F3	Optimal $C_d$ from PA_NoPT3	Same $C_d$ as the nowcast
SWL_F4	Optimal $C_d$ from PA_PT1	Eq. (6)
SWL_F5	Optimal $C_d$ from PA_PT1	Same $C_d$ as the nowcast

tion coefficients vary in the range from 0.75 to 0.8. Both the average RMS errors and correlation coefficients do not change much as the forecast hour increases. For the experiment with data

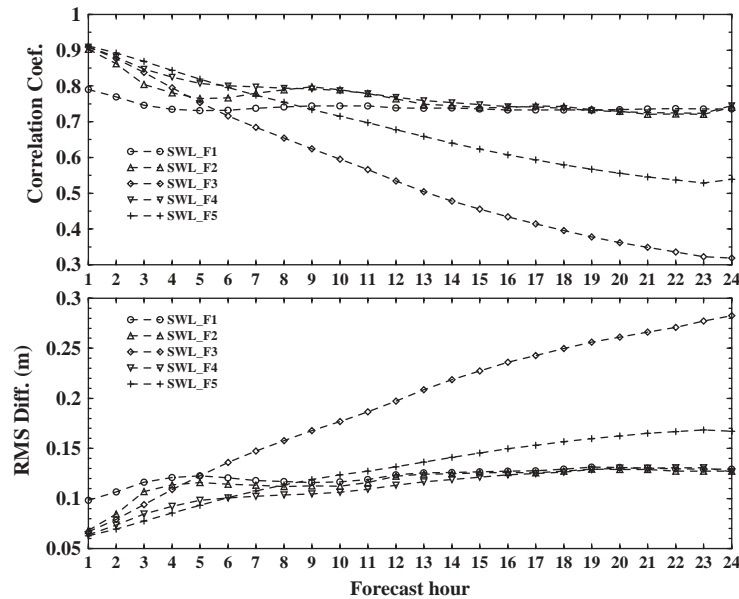


Fig. 11. Average correlation coefficients and RMS errors for each forecast hour between the observed and forecasted subtidal water levels over 18 stations from the nowcast/forecast experiments. See Table 2 for explanation of five cases shown.

assimilation in the nowcast (without penalty terms) but using the Large and Pond formulation for  $C_d$  (Eq. (6)) in the forecast (SWL\_F2), the RMS errors are about 3 cm less than for SWL\_F1 in the first 2 h and 0.5 cm less from hour 3 to hour 11. When the forecast time is greater than 11 h, differences of the RMS errors between SWL\_F1 and SWL\_F2 are insignificant. For the experiment with data assimilation but applying the optimal  $C_d$  of the previous day to the next 24 h forecast (SWL\_F3), the RMS errors are slightly smaller than that of SWL\_F2 in the first 4 h. However, the RMS errors then increase very fast and they are even much larger than that of SWL\_F1 when the forecast time is greater than 6 h. These results indicate that, on the average, the improvement of subtidal water level forecasts by applying the data assimilation without penalty terms is mostly limited to the first 3 h. After 3 h, the improvement in the subtidal water level forecasts is insignificant. The subtidal water level forecasts made by extending the optimal  $C_d$  of the previous day's nowcast to the following day's forecasts become even worse than those without data assimilation

after the 5th hour. By introducing penalty terms into the cost function formulation (SWL\_F4 and SWL\_F5), the RMS error becomes smaller than that of SWL\_F2, and they are about 3 cm smaller than that of SWL\_F1 in the first 5 h. For SWL\_F5, the RMS errors become larger than that of SWL\_F1 after about 8 h. The results of SWL\_F3 and SWL\_F5 indicate that the value of the optimal  $C_d$  from the previous day's nowcast cannot be simply applied to the next day's forecasts. It was expected that the adjustment to  $C_d$  correct for errors in the changing wind field would vary day to day, but the size of such adjustments is apparently large enough so that trying to use one day's calculated  $C_d$  for the following day is actually worse than sticking with the Large and Pond  $C_d$ , at least a few hours into the forecast.

The average improvement percentage of subtidal water level forecasts by the data assimilation technique over 18 stations for each forecast hour is calculated as

$$P = \frac{\overline{\text{RMS}}_{NoDA} - \overline{\text{RMS}}_{DA}}{\overline{\text{RMS}}_{NoDA}} 100\%, \quad (11)$$

where  $P$  is average improvement,  $\overline{\text{RMS}}_{\text{NoDA}}$  and  $\overline{\text{RMS}}_{\text{DA}}$  are the average RMS errors without (SWL\_F1) and with data assimilation, respectively. Fig. 12 indicates that the percentage of SWL\_F2 (without penalty terms) decreases faster than that of SWL\_F4 (with penalty terms). A drop to a 10% improvement takes place in the first 3 h for SWL\_F2 and in the first 9 h for SWL\_F4. The improvement of SWL\_F4 is greater than that of SWL\_F2. Therefore, adding the penalty terms in the cost function formulation to smooth optimal wind drag coefficients leads to the most improved forecast results.

The RMS errors of the subtidal water level forecast from SWL\_F4 as a function of forecast hour at the 18 stations are listed in Table 3. The RMS errors in 24-h forecast cycle are less than 14 cm except at Springmaid, Charleston and Fort Pulaski, and are generally less than 10 cm during the first 6 h. The maximum RMS error of 21 cm occurred around Charleston, South Carolina after 20 h. However, the RMS errors of the nowcast near Charleston (see Fig. 10) are not significantly larger than those of the other stations. In examining the Eta forecast and EDAS-analyzed

surface wind fields (Fig. 13), we found that the Eta forecast and EDAS-analyzed wind fields are very different near Charleston during Julian days 320–322, 328–329 and 360–362. In those days, the wind forecasts produced extremely large subtidal water level forecasts at Charleston, Springmaid and Fort Pulaski, which were different from the observations and resulted in the large RMS errors in that region.

## 6. Conclusions

A water level data assimilation system based on the two-dimensional linear POM for the East Coast of the United States has been developed to improve subtidal water level simulation through adjusting the wind drag coefficient by dynamical assimilation of subtidal water levels into the numerical model. The simulated wind-driven subtidal water levels from the linear two-dimensional POM are in good agreement with the observed subtidal water levels at coastal water level gauge stations. The only exception is at Cape Hatteras, probably due to the effect of the Gulf

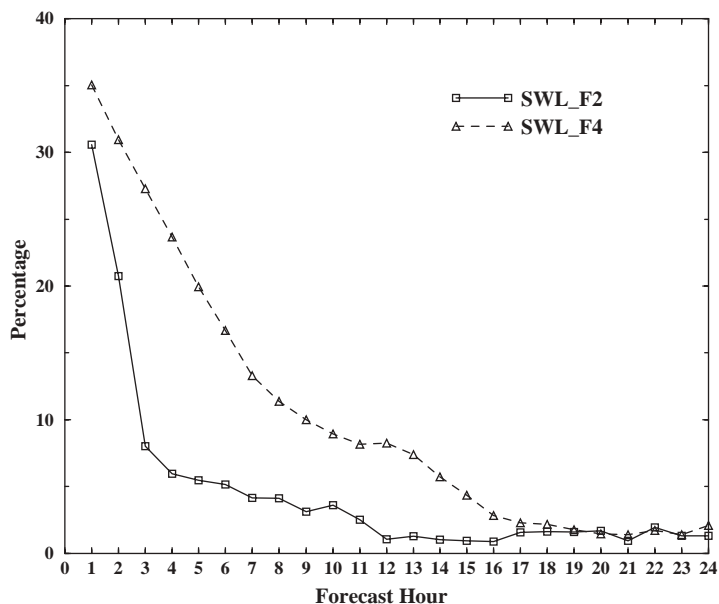


Fig. 12. Average improvement percentage in subtidal water level forecasts (Eq. (11)) by applying water level data assimilation with and without penalty terms.

Table 3

RMS errors for each forecast hour at 18 water level gauge stations based on 110 days subtidal water level forecasts with the experiment SWL\_F4. See Fig. 2 for names of water level stations

Hour	1	2	3	4	5	6	7	8	9	10	11	12	13	14	15	16	17	18
1	6.6	6.6	6.2	4.3	4.8	4.1	5.6	4.6	6.1	5.2	8.0	7.5	7.0	8.8	8.3	7.3	6.9	6.8
2	7.4	6.8	7.0	4.8	5.3	4.6	6.0	5.6	7.6	6.4	9.0	7.4	8.0	10.2	10.7	9.4	9.0	7.2
3	7.4	7.2	7.3	5.6	6.3	5.5	6.9	8.1	8.6	7.5	10.3	8.6	9.4	11.6	12.5	12.3	9.5	7.5
4	7.8	7.5	8.2	6.7	7.7	6.9	8.4	9.3	6.8	7.5	9.5	10.7	10.0	13.9	14.2	14.3	9.3	7.2
5	8.4	8.0	8.3	7.4	9.5	8.2	10.1	8.6	7.0	7.2	9.4	10.9	10.8	15.5	16.1	14.5	9.5	7.3
6	8.0	8.2	8.4	7.9	10.9	8.8	10.9	8.8	7.6	7.8	9.8	11.1	10.6	14.9	15.0	14.4	10.2	7.4
7	7.2	7.8	8.9	8.5	10.8	9.6	10.8	9.3	8.1	8.6	10.2	11.2	10.4	14.5	15.4	15.2	10.4	7.3
8	7.0	7.8	8.8	8.8	10.8	9.6	10.5	9.7	8.3	8.9	10.6	11.2	10.8	14.7	16.5	15.3	10.0	7.4
9	6.6	7.3	8.9	9.0	10.9	9.4	10.5	10.8	8.6	8.8	10.6	11.5	10.9	14.9	16.9	14.8	10.0	7.6
10	7.0	7.3	8.3	9.3	10.7	9.6	10.7	11.4	9.1	8.9	10.8	11.8	11.2	15.8	16.9	14.1	10.3	7.7
11	7.4	7.5	8.4	9.4	10.5	9.8	10.7	11.6	9.1	9.3	10.9	12.3	11.3	17.1	17.6	15.0	10.7	8.0
12	7.5	7.9	8.6	9.6	10.8	10.1	10.7	11.7	9.7	9.9	11.3	12.3	11.6	17.9	18.4	16.8	11.2	8.2
13	7.9	8.3	9.3	9.8	11.2	10.6	11.0	11.8	10.1	10.1	11.6	12.5	11.8	17.6	18.7	17.7	11.7	8.3
14	8.3	8.5	9.6	9.9	11.4	10.7	11.4	12.2	10.0	10.1	11.7	13.0	12.1	17.4	19.0	18.0	12.1	8.4
15	9.2	8.7	9.3	10.3	11.5	11.1	11.7	12.9	10.3	10.4	11.5	13.4	12.4	17.2	19.5	18.1	12.2	8.3
16	9.6	9.0	9.6	10.6	11.9	11.6	11.7	13.1	10.9	10.9	11.8	13.5	12.5	17.4	19.5	18.5	12.1	8.3
17	9.5	9.2	9.9	10.7	12.3	11.9	11.8	13.0	11.3	11.1	12.1	13.4	12.6	17.6	19.3	18.5	12.1	8.5
18	9.6	9.2	10.4	10.7	12.5	11.9	12.0	12.8	11.5	11.4	12.1	13.6	12.7	17.9	19.5	18.5	12.5	8.7
19	10.1	9.3	10.8	10.6	12.5	11.8	12.4	12.9	11.7	11.7	12.1	13.8	12.9	18.5	20.4	18.9	13.1	8.8
20	10.6	9.4	10.7	10.4	12.3	11.5	12.4	13.0	11.7	11.7	12.0	13.9	12.9	18.9	21.2	19.3	13.4	9.0
21	11.0	9.6	10.7	10.5	12.1	11.4	12.2	12.8	11.9	11.8	12.0	13.8	12.9	18.9	21.3	19.7	13.5	8.9
22	11.2	9.6	10.8	10.7	11.9	11.4	11.9	12.6	12.1	12.1	12.1	13.7	12.9	18.9	21.1	20.0	13.3	8.9
23	11.4	9.8	11.1	10.6	11.9	11.4	11.7	12.5	12.1	12.2	12.0	13.6	12.9	18.7	21.0	20.0	13.5	9.1
24	11.5	9.8	11.2	10.7	11.8	11.3	11.6	12.4	12.0	12.2	12.0	13.7	12.9	18.6	21.1	20.1	14.0	9.1

Stream which is not included in the model. This shows that in the US East Coast region surface wind forcing is the predominant factor in low-frequency water level variations.

The correct gradient of the cost function is efficiently obtained by the adjoint approach. A set of identical twin experiments with model-generated pseudo-observations shows that the true solution of the control variable can be exactly recovered for both single and multiple control variable experiments, even if the first guess of the control variable is far from its true solution. The rate of convergence is very fast, taking only a few iterations. The identical twin experiments also show that water level observational errors affect the convergence rate and performance of the minimization procedure.

The performance of the adjoint data assimilation system in the application using real water level data indicates that the simulated subtidal water

levels with data assimilation have been improved even with one control variable. From comparison among a number of the experiments, it is found that the most accurate simulated subtidal water levels are obtained from the experiment with 16 control variables (using  $x$  and  $y$  pairs in eight regions). In this case, the correlation coefficients are greater than 0.93 and the RMS errors are less than 5.3 cm at 18 water level gauge stations. This experiment demonstrates that both the magnitude and direction of wind stress need to be adjusted in order to minimize the cost function. The penalty terms should also be included in the cost function to assure the smoothness of the estimated optimal wind drag coefficients in space and time. Results from the experiments with the penalty terms indicate that the estimated optimal values of  $C_d$  are smoother in space and time than that without the penalty terms. However, the RMS error differences between the simulated subtidal water

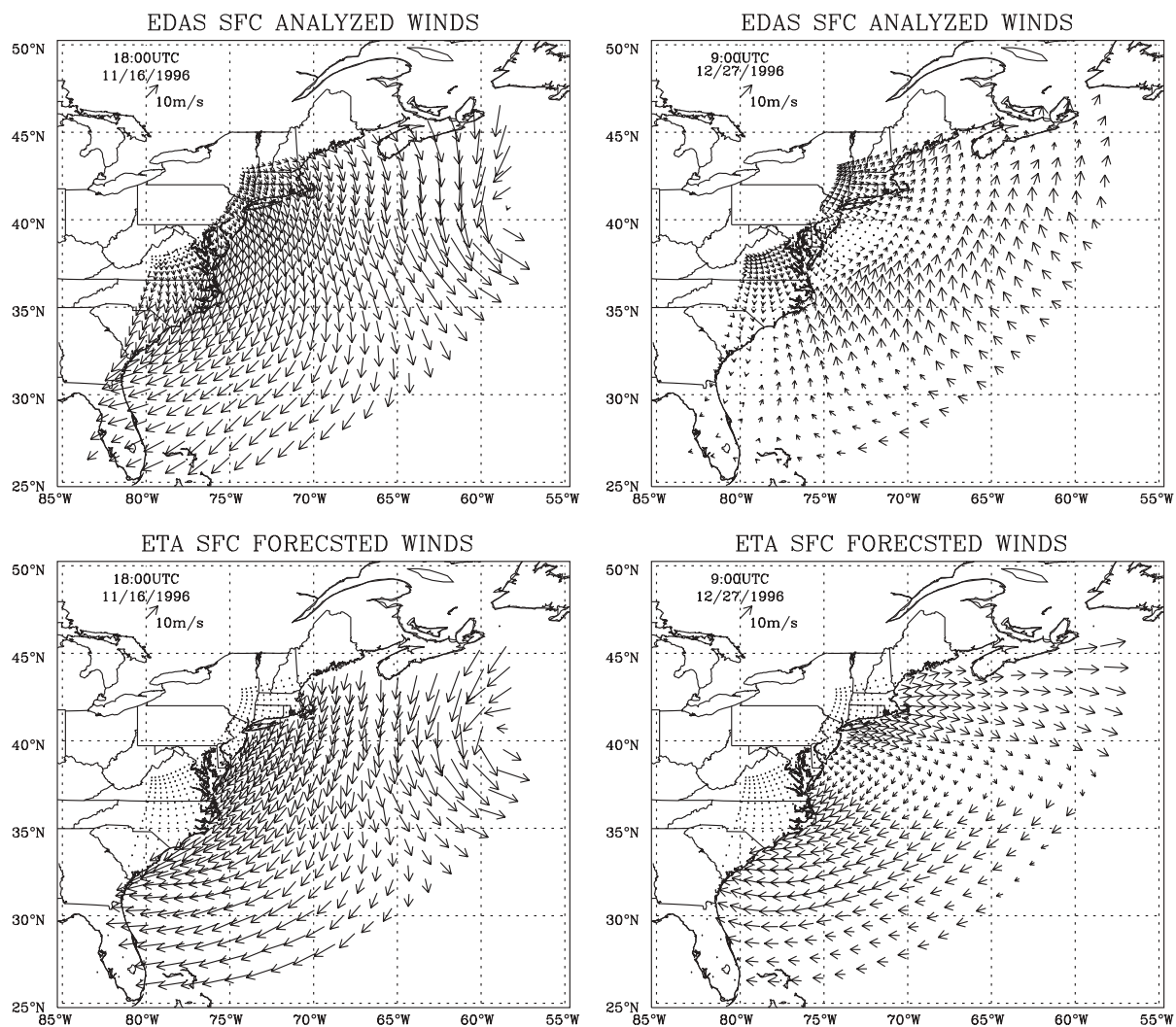


Fig. 13. Comparison between the EDAS-analyzed and Eta-forecasted wind fields for two different times (left panels, 11/16/1996; right panels, 12/27/1996). Upper panels are EDAS-analyzed wind fields. Lower panels are Eta-forecasted wind fields.

levels with and without penalty terms are generally very small except near Charleston. Thus, adding the penalty terms leads to smoother solutions that still preserve the physical features of subtidal water levels. In addition, water level forecasts were improved when penalty terms were used in the nowcasts that were used to initialize the following forecasts

The nowcast/forecast experiments demonstrate that the average RMS errors of the subtidal water level forecasts over the 18 water level gauge

stations without data assimilation vary from 8.8 to 12 cm, and the average correlation coefficients vary from 0.76 to 0.81. The most of the improvement in the subtidal water level forecasts by applying data assimilation into the nowcast/forecast system occur within the first 6 h, with no significant differences between the water level forecasts with and without data assimilation thereafter. This indicates that the impact of the initial conditions from the nowcast on the next day's forecast is limited to the first 6 h. The

optimal values of  $C_d$  from the previous day's water level data assimilation cannot be directly applied in the next day's water level forecasts due to the changes in the surface wind fields. These optimal values may only be reasonably extended about 3–6 h into forecasts. More experiments should be performed to find a way of predicting the next day's  $C_d$  based on the optimal values of  $C_d$  of the previous day in order to improve the next day's water level forecast.

Due to the limitation in the number and spatial distribution of the available water level observations (the real-time water level data are available at only 18 water level gauge stations within the model domain), a large number of control variables could not be used in the data assimilation process. Sea surface height data from satellite altimeters might help to alleviate this limitation. Combining water level gauge observations, which are long-term and frequently sampled in time, with the altimetry data, which cover wide spatial areas but are infrequently sampled in time, could possibly improve the resolution of the wind drag coefficients, and then improve the accuracy of nowcast/forecast systems.

## Acknowledgements

We thank Dr. Yuanfu Xie for his helpful guidance in the adjoint equation construction. The authors also thank the anonymous reviewers from *Continental Shelf Research* for their valuable comments on the manuscript. Dr. Frank Aikman and Dr. Kurt Hess are appreciated for their careful and constructive comments during the internal reviews. Aijun Zhang conducted this work while he was a UCAR visiting scientist in CSDL.

## References

- Aikman, F., Mellor, G.L., Ezer, T., Sheinin, D., Chen, P., Breaker, L., Bosley, K., Rao, D.B., 1996. Towards an operational nowcast/forecast system for the US East Coast. In: Malanotte-Rizzoli, P. (Ed.), *Modern Approaches to Data Assimilation in Ocean Modeling*. Elsevier Oceanographic Series, Vol. 61. Elsevier, New York, pp. 347–376.
- Baptista, A.M., Wilkin, M., Pearson, P., Turner, P., McCandlish, C., Barrett, P., Das, S., Sommerfield, W., Qi, M., Nangia, N., Jay, D., Long, D., Pu, C., Hunt, J., Yang, Z., Myers, E., Darland, J., Farrenkopf, A., 1998. Towards a multi-purpose forecast system for the Columbia River Estuary. Ocean Community Conference '98, Baltimore, MD.
- Bennett, A.F., 1985. Array design by inverse method. *Progress in Oceanography* 15, 129–156.
- Bennett, A.F., McIntosh, P.C., 1982. Open ocean modeling as an inverse problem: tidal theory. *Journal of Physical Oceanography* 12, 1004–1018.
- Black, T.L., 1994. The new NMC mesoscale Eta model: description and forecast examples. *Weather Forecasting* 9, 265–278.
- Blumberg, A.F., Mellor, G.L., 1987. A description of a three-dimensional coastal ocean circulation model. In: Heaper, N.S. (Ed.), *Three Dimensional Coastal Ocean Models*. American Geophysical Union, Washington, DC, pp. 1–16.
- Courtier, P., Talagrand, O., 1990. Variational assimilation of meteorological observations with the direct and adjoint shallow-water equations. *Tellus* 42A, 531–549.
- Das, S.K., Lardner, R.W., 1991. On the estimation of parameters of hydraulic models by assimilation of periodic tidal data. *Journal of Geophysical Research* 96 (C8), 15187–15196.
- Gross, T.F., Bosley, K.T., Hess, K.W., 2000. The Chesapeake Bay operational forecast system (CBOFS): technical documentation. NOAA Technical Report OCS/CO-OPS 1, 69pp.
- Lardner, R.W., 1993. Optimal control of open boundary conditions for a numerical tidal model. *Computer Methods in Applied Mechanics and Engineering* 102, 367–387.
- Lardner, R.W., Song, Y., 1995. Optimal estimation of eddy viscosity and friction coefficients for a quasi-three-dimensional numerical tidal model. *Atmosphere-Ocean* 33 (3), 581–611.
- Lardner, R.W., Al-Rabeh, A.H., Gunay, N., 1993. Optimal estimation of parameters for a two-dimensional hydrodynamical model of the Arabian Gulf. *Journal of Geophysical Research* 98, 18229–18242.
- Large, W.G., Pond, S., 1981. Open ocean momentum flux measurements in moderate to strong winds. *Journal of Physical Oceanography* 11, 324–336.
- Le Dimet, F.X., Talagrand, O., 1986. Variational algorithms for analysis and assimilation of meteorological observations: theoretical aspects. *Tellus* 38A, 97–110.
- Liu, D., Nocedal, J., 1989. On the limited memory BFGS method for large scale optimization. *Mathematical Programming* B 45, 503–528.
- Malanotte-Rizzoli, P., Tziperman, E., 1996. The oceanographic data assimilation problem: overview, motivation and purposes. In: Malanotte-Rizzoli, P. (Ed.), *Modern Approaches to Data Assimilation in Ocean Modeling*. Elsevier Science, New York, pp. 3–17.
- Morse, P., Feshbach, H., 1953. *Method of Theoretical Physics: Part I*. McGraw-Hill, New York.

- National Geophysical Data Center, 1985. Worldwide gridded bathymetry, DBDB5 5 minute latitude/longitude grid. Data announcement 85-MGG-01, NOAA/NGDC, Boulder, CO.
- National Geophysical Data Center, 1988. NOS Hydrographic data base-expanded, digital bathymetric data for US coastal waters. Data announcement 87-MGG-12, NOAA/NGDC, Boulder, CO.
- Noble, M.A., Butman, B., 1979. Low-frequency wind-induced sea level oscillations along the East Coast of North America. *Journal of Geophysical Research* 84 (C6), 3227–3236.
- Panchang, V.G., O'Brien, J.J., 1989. On the determination of hydraulic model parameters using the adjoint state formulation. In: Davies, A.M. (Ed.), *Modeling Marine Systems*. CRC Press, Boca Racon, FL, pp. 6–18.
- Rogers, E., Deaven, D.G., DiMego, G.J., 1995. The regional analysis system for the operational Eta model: original 80-km configuration and recent changes. *Weather Forecasting* 10, 810–825.
- Sasaki, Y., 1970. Some basic formalisms in numerical variational analysis. *Monthly Weather Review* 98 (12), 875–883.
- Seiler, U., 1993. Estimation of open boundary conditions with the adjoint method. *Journal of Geophysical Research* 98, 22855–22870.
- Spitz, Y.H., 1995. A feasibility study of dynamical assimilation of tide gauge data in the Chesapeake Bay. Ph.D. Thesis, Old Dominion University, 167pp.
- Wang, D.P., 1979. Low-frequency sea level variability on the Middle Atlantic Bight. *Journal of Marine Research* 37683–37697.
- Yu, L., O'Brien, J.J., 1991. Variational estimation of the wind stress drag coefficient and the oceanic eddy viscosity profile. *Journal of Physical Oceanography* 21, 709–719.
- Yu, L., O'Brien, J.J., 1992. On the initial condition in parameter estimation. *Journal of Physical Oceanography* 22, 1361–1364.
- Zhang, A., Parker, B.B., Wei, E., 2002. Development of an east coast water level data assimilation model. US Department of Commerce, NOAA Technical Report, NOS CS13, Silver Spring, Maryland, 102pp.
- Zou, X., Navon, I.M., Le Dimet, F.X., 1992. Incomplete observations and control of gravity waves in variational data assimilation. *Tellus* 44A, 273–296.